Single-Pulse Phase-Contrast Nonlinear Raman Spectroscopy

Dan Oron, Nirit Dudovich, and Yaron Silberberg

Department of Physics of Complex Systems, Weizmann Institute of Science, Rehovot 76100, Israel

(Received 11 July 2002; published 17 December 2002)

High spectral resolution nonlinear vibrational spectroscopy with a single ultrashort pulse is demonstrated on a variety of samples. The spectral data are obtained by shaping the excitation pulse in order to control the relative phase between the weak resonant signal and the strong nonresonant background, in analogy with phase-contrast microscopy techniques. This is unlike the more conventional approach to nonlinear spectroscopy, in which the nonresonant background is reduced to a minimum. By measuring the spectrum of the coherent anti-Stokes Raman signal, it is possible to infer the vibrational energy levels in a band spanning almost an entire octave.

DOI: 10.1103/PhysRevLett.89.273001 PACS numbers: 32.80.Qk, 42.65.Dr, 78.47.+p, 82.53.Kp

In coherent nonlinear spectroscopy, the sample is probed by measuring processes of energy exchange between photons interacting with it [1]. Since these processes typically have a quadratic or a cubic dependence on the excitation field intensity, illumination by ultrashort pulses is favored for driving them.

Perhaps the most common nonlinear spectroscopy method is coherent anti-Stokes Raman scattering (CARS), a four-wave mixing process involving the generation of a coherent vibration in the probed medium [2]. In CARS, a pump photon ω_p, a Stokes photon ω_s, and a probe photon ω_{pr} mix to emit a signal photon $\omega_p - \omega_s + \omega_{pr}$. The energy level diagram of this process is schematically plotted in Fig. 1(a). Resonant enhancement occurs when the energy difference $\omega_p - \omega_s$ coincides with a vibrational level of the medium. Typically, two narrow-band sources at ω_p and at ω_s are used to generate a signal at $2\omega_p - \omega_s$ (in this case, $\omega_{pr} = \omega_p$). The use of a narrow-band probe and a broad-band Stokes beam has enabled simultaneous measurement of an entire band of the Raman spectrum (multiplex CARS) [2]. Coherent Raman processes have become a valuable tool in femtosecond time-resolved spectroscopy, combustion studies, and condensed-state spectroscopy. CARS has recently become a favorable method for multiphoton depth-resolved microscopy [3–5].

Recently, we have demonstrated high-spectral resolution single-pulse coherently controlled CARS spectroscopy and microscopy [6] using pulses of a duration of the order of 20 fs, having a bandwidth larger than the vibrational energy of the measured levels. Applying coherent-control techniques, Raman levels were excited selectively with a resolution of about 30 cm^{-1}, nearly 2 orders of magnitude better than the pulse bandwidth. The single-pulse CARS scheme requires a single fixed-frequency ultrafast laser source. This is advantageous compared with the standard multibeam excitation scheme, which requires synchronized tunable sources.

Working with such short pulses, however, introduces a very large nonresonant background, which accompanies the resonant Raman signal. This background, which is due to the instantaneous nonlinear electronic response, is a common problem in coherent nonlinear spectroscopy. It increases as shorter excitation pulses, having a higher peak intensity, are used [5]. Because of the coherent nature of CARS, the resonant and the nonresonant contributions interfere with each other. The nonresonant background thus alters the CARS line shape [1], and can be detrimental to the ability to spectrally resolve resonant transitions. For singly resonant processes, such as CARS, the two contributions appear in quadrature, due to the phase shift induced by the resonance. When the resonant signal is accompanied by a strong nonresonant background in quadrature, the total intensity variation due to the resonant signal depends on the resonant signal intensity only to second order, resulting in a poor

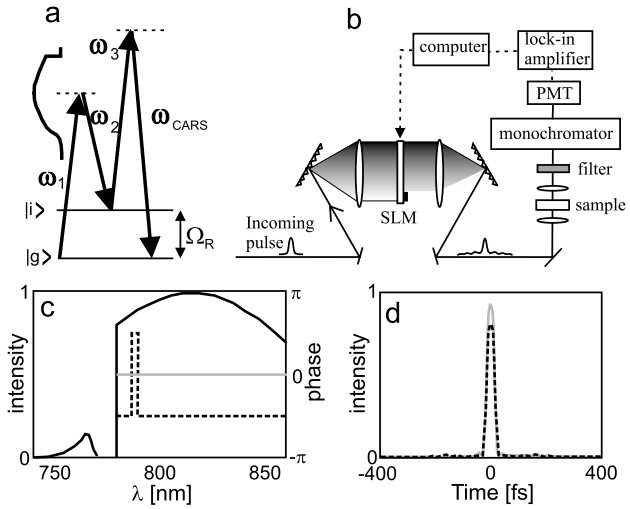

FIG. 1. (a) Energy level diagram of the CARS process. Shown also is the single-pulse excitation spectrum. (b) Outline of the experimental setup. (c) Schematic drawing of the excitation pulse spectral intensity (solid black line) and spectral phase of a transform limited pulse (gray line) and a phase-gate shaped pulse (dashed line). Also shown is the spectral region where the CARS signal is measured. (d) Temporal intensity of a transform limited pulse (gray line) and a phase-gate shaped pulse (dashed line).

signal-to-background ratio. It is thus crucial to reduce the nonresonant background to a minimum in order to measure the resonant contribution.

In a CARS process, there are several methods to reduce this background term. The simplest one is to use longer pulses, whose duration is of the order of the vibrational level lifetime. This also leads to a high-spectral resolution, since the spectral resolution limit is usually due to the bandwidth of the excitation beams, but requires tunable synchronized ultrafast sources [5]. Further reduction can be achieved by using a polarization configuration measuring a component of the polarizability which contains only resonant terms [7]. Another option is the coherent subtraction of a separate fully nonresonant signal with an appropriate amplitude [8]. Coherent-control methods combined with broad-band illumination have been demonstrated as a more sophisticated means to obtain high-spectral resolution with a low nonresonant background [9]. In the aforementioned single-pulse CARS experiments [6], the nonresonant background was reduced, using coherent-control techniques, by nearly 2 orders of magnitude, to a level substantially below the resonant signal.

We suggest here a new method to obtain spectral data while greatly relaxing the need to reduce the nonresonant background by using it as a local oscillator with which the resonant contribution is measured in heterodyne. Such a scheme is useful when the nonresonant background is much stronger than the resonant signal (i.e., weak Raman transitions probed by short pulses) and is particularly attractive for single-pulse CARS. This is done by shifting the spectral phase of the excitation pulse by π in a narrow frequency range, inducing a $\pm\pi/2$ phase shift to the resonant signal relative to the nonresonant background with which it was initially in quadrature. The small intensity variation due to the resonant signal is amplified by heterodyne detection with the strong nonresonant background. High-resolution spectroscopy is thus enabled even though the nonresonant signal level is almost unchanged. The suggested scheme is analogous to Zernike's widely used scheme of phase-contrast microscopy [10], in which the high spatial frequencies are imaged by retarding them relative to the strong low frequency background, with which they are initially in quadrature.

While in the following we focus on single-pulse CARS spectroscopy, the suggested technique can be applied to other nonlinear optical processes excited by broadband pulses, such as infrared-visible sum-frequency generation microspectroscopy [11].

The nonlinear polarization producing the CARS signal driven by an electric field whose spectrum is $\epsilon(\omega)$ can be approximated for nonresonant transitions [12]:

$$P_{nr}^{(3)}(\omega) \propto \int_0^\infty d\Omega\, \epsilon(\omega - \Omega) A(\Omega), \tag{1}$$

where $A(\Omega) = \int_0^\infty d\omega \epsilon^*(\omega - \Omega)\epsilon(\omega)$ is the second order polarization driving molecular vibrations. For a singly resonant Raman transition through an intermediate level $|i\rangle$ at an energy of $\hbar\Omega_R$ and a bandwidth Γ we obtain the following:

$$P_r^{(3)}(\omega) \propto \int_0^\infty d\Omega\, \frac{\epsilon(\omega - \Omega)}{(\Omega_R - \Omega) + i\Gamma} A(\Omega). \tag{2}$$

Phase-only pulse shaping, used in our experiments, simply means multiplication of the electric field in Eqs. (1) and (2) by a phase function $\exp[i\Phi(\omega)]$. In our experiments we apply narrow-band features in the high-energy (short wavelength) end of the excitation pulse, inducing sharp changes in the phase of $\epsilon(\omega - \Omega)$. Such changes, however, hardly modify $A(\Omega)$ since the energy content in a narrow spectral band part is negligible compared with the entire pulse energy. The resonant signal from a level Ω_R at any given frequency ω, is due to a rather narrow-band probe, centered at $\omega - \Omega_R$. In contrast, the nonresonant background is a coherent sum contributed by a large portion of the pulse bandwidth. Thus, phase changes over a narrow spectral band, while dramatically affecting the phase of the resonant component, hardly modify the phase of the nonresonant one, making a suitable local oscillator. Measuring the total CARS spectrum, the interference pattern between the resonant signal and the nonresonant background can be interpreted to reveal the vibrational energy level diagram.

To demonstrate single-pulse phase-contrast CARS spectroscopy, we considered Raman transitions in several simple molecules. The impulsive excitation is driven by 20 fs full width at half maximum (FWHM) transform-limited pulses, centered at 815 nm (corresponding to a bandwidth of about 70 nm), generated by a Ti:sapphire laser. Spectral phases were applied by a programmable pulse shaper, which includes a liquid crystal spatial light modulator (SLM) [13]. The spectral resolution, determined by the spot size at the Fourier plane, is 0.5 nm (equivalent to about 8 cm^{-1}). Wavelengths shorter than 780 nm are blocked at the Fourier plane as they spectrally overlap the CARS signal [as shown in Fig. 1(c)]. A spectral band between 780 and 855 nm (corresponding to an energy span of 1100 cm^{-1}) was used to induce the CARS process. The shaped pulse was focused into the sample using a numerical aperture (NA) = 0.2 objective. The CARS signal was filtered by both a 40 nm FWHM bandpass filter centered at 750 nm, and a computer-controlled monochromator with a spectral resolution of 0.5 nm (equivalent to about 8 cm^{-1}), and measured with a photomultiplier tube and a lockin amplifier. An outline of the experimental setup is shown in Fig. 1(b). The measurable Raman energy range of our system is about 400–700 cm^{-1}, typical of carbon-halogen bond stretching. The lower limit is determined by the need to filter out the excitation pulse. The upper limit is dictated by the excitation pulse bandwidth.

High-resolution spectroscopy is demonstrated by comparing the CARS spectra obtained with two different pulse shapes. One is a transform-limited pulse, and the other is a pulse whose spectral phase has been shifted by π in a narrow band of about 1.5 nm at 790 nm. This shape will be referred to as a π phase gate. The pulse spectrum, along with the two spectral phases is plotted in Fig. 1(c). The temporal envelope of the two pulses is shown in Fig. 1(d). As can be seen, the narrow π phase gate hardly affects the pulse, merely reducing the peak intensity by about 15%. The main effect of the phase gate on the nonresonant background should therefore be a factor of $(0.85)^3 \approx 1/2$ decrease in total intensity. The resonant CARS signal, however, behaves differently due to its narrow spectral response and the rapid phase variation of the probing field $\epsilon(\omega - \Omega)$ around the phase gate.

This effect is demonstrated in the numerical simulation results shown in Fig. 2. The spectrum of both the resonant and the nonresonant contributions, along with the relative phase between the two for a transform-limited pulse illuminating iodomethane (resonant at 523 cm^{-1}) is shown on the top part of Fig. 2(a). The resulting total CARS intensity is shown at the bottom. As can be seen, the nonresonant background spectrum monotonically decreases towards higher energies, while the resonant signal resembles the excitation pulse spectrum, shifted by the Raman level energy. The relative phase between the two is nearly constant at about $\pi/2$, rising to about π below 749 nm. Note that a peak is formed in the resonant spectrum at 749 nm, which corresponds to the spectral location of the blocker on the excitation pulse, shifted by the Raman level energy, due to a transient enhancement effect [12]. Figure 2(b) presents similar spectra of iodomethane, this time illuminated by the shaped pulse. Three effects can be seen. First, as expected, there is some reduction of the nonresonant background. Second, two new peaks appear in the resonant spectrum, at both ends of the phase gate. These are due to a transient enhancement effect demonstrated previously in standard multibeam CARS [12]. The most dominant effect, however, is the induced change in the relative phase between the resonant signal and the nonresonant background [14]. Because of the phase gate, the two interfere constructively at the high-energy side of the gate, generating a peak in the CARS spectrum, and destructively at the low-energy side, generating a dip in the CARS spectrum, as seen in the bottom part of Fig. 2(b). This feature in the CARS spectrum is generated by heterodyning the weak resonant signal with the nonresonant background. Note that due to amplification by this heterodyne effect the CARS intensity variation is an order of magnitude stronger than the intensity of the resonant signal itself. This feature determines the energy of the vibrational level with an accuracy of the phase gate width. In our experiments the phase gate consisted of three pixels on the SLM, corresponding to about 25 cm^{-1}, about 40 times better than the excitation pulse width [15]. Measured normalized spectra of methanol (nonresonant signal only), both for transform-limited pulses and for shaped pulses are shown in Fig. 3(a). Similar spectra of iodomethane are shown in Fig. 3(b). The peak-dip feature due to the resonant contribution at 523 cm^{-1} is evident in the iodomethane spectrum, while the normalized methanol spectrum remains nearly unchanged. The sharp decrease of the CARS spectrum at wavelengths above 765 nm is merely due to the filtering of the excitation spectrum.

The Raman level structure can be easily extracted from the measured spectrum by considering the normalized spectral intensity variation of the CARS signal

$$f(\Omega) = -\frac{I(\omega_g + \Omega - \Delta/2) - I(\omega_g + \Omega + \Delta/2)}{\int_{\omega_g+\Omega-\Delta/2}^{\omega_g+\Omega+\Delta/2} I(\omega)d\omega}, \quad (3)$$

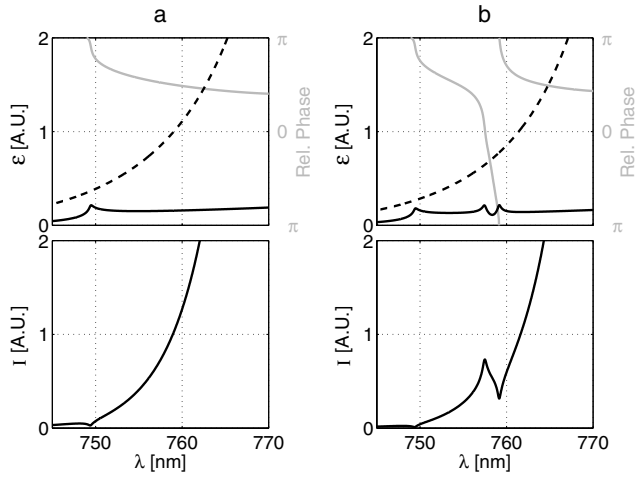

FIG. 2. The top images show the calculated CARS electric field as a function of frequency for the resonant signal (solid line) and the nonresonant background (dashed line) for iodomethane. Also shown is the relative phase between the two. The bottom images show the calculated resulting CARS spectrum. (a) Transform-limited pulse. (b) Phase-gate shaped pulse.

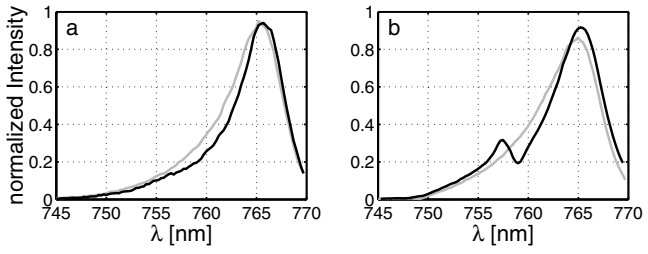

FIG. 3. Normalized CARS spectra for a transform limited pulse (gray line) and a phase-gate shaped pulse (black line) for (a) Methanol (nonresonant signal only). (b) Iodomethane (resonant at 523 cm^{-1}). While in (a) the spectra look similar, a peak and a dip appear only in the iodomethane spectrum using a shaped pulse (b).

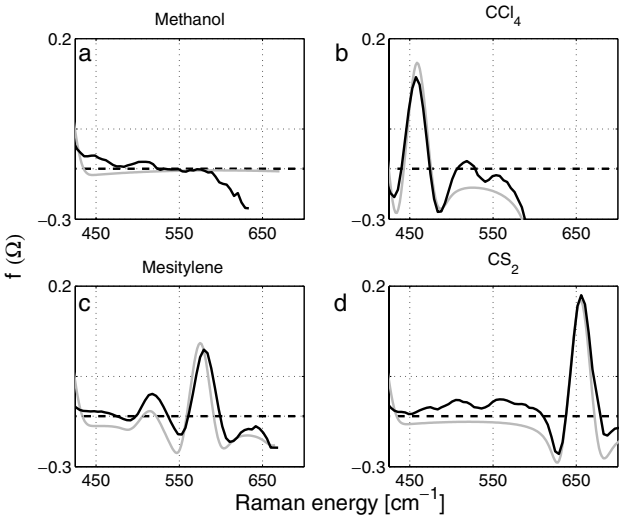

FIG. 4. Vibrational energy level structure $f(\Omega)$ as derived from the measured spectra (black lines) along with the calculation predictions (gray lines). (a) Methanol (nonresonant signal only). (b) Carbon tetrachloride (resonant at $459\,cm^{-1}$). (c) Mesitylene (weaker resonance at $515\,cm^{-1}$, stronger resonance at $575\,cm^{-1}$). (d) Carbon disulfide (resonant at $652\,cm^{-1}$).

where ω_g is the cental frequency of the phase gate and Δ its width. The normalization is required to compensate for the decrease in the nonresonant background towards higher energies. Plots of $f(\Omega)$ derived from the measured CARS spectra are given in Fig. 4 for several materials, along with simulation predictions. A nearly flat line is observed for methanol, having no Raman level in this range [Fig. 4(a)]. The $459\ cm^{-1}$ level of carbon tetrachloride is easily observed in Fig. 2(b). For mesitylene [Fig. 4(c)], having two Raman levels at $515\ cm^{-1}$ and $575\ cm^{-1}$ two well-separated peaks can be seen. At the high-energy end, the $652\ cm^{-1}$ level of carbon disulfide is shown in Fig. 4(d).

The benefits of broad-band excitation can be fully exploited when attempting to detect materials with several vibrational bands in the measured energy range. In this case, a spectral phase mask with multiple phase gates at appropriate locations can be used to generate a large coherent spectral feature in the CARS spectrum, due to the constructive interference of the resonant contributions from the various levels.

In summary, we have presented a novel method for nonlinear spectroscopy with broad-band pulses. In this method, the strong nonresonant background accompanying all nonlinear processes is used as a controllable local oscillator, greatly relaxing requirements for its suppression. By measurement of the CARS spectrum, all vibrational energy levels in a range spanning nearly an entire octave can be simultaneously mapped in a single measurement, as in recent multiplex CARS experiments. This is in contrast to the single-pulse CARS spectroscopy based on selective excitation of Raman levels [6], where spectral data are obtained by switching between pulse shapes. While in the presented scheme we measure the CARS spectrum, resulting in a weaker signal than in Ref. [6], it is advantageous since it is insensitive to power fluctuations of the excitation beam, which were the main source of noise in Ref. [6]. Using state-of-the-art Ti:sapphire lasers, single-pulse Raman spectra in the fingerprint region ($1000–1500\ cm^{-1}$) can be readily measured.

Financial support of this research by the Israel Science Foundation and by the German BMBF is gratefully acknowledged.

[1] M. D. Levenson, *Introduction to Nonlinear Laser Spectroscopy* (Academic Press, New York, 1982), p. 136.
[2] *Infrared and Raman Spectroscopy*, edited by B. Schrader (VCH, Weinheim, 1995).
[3] A. Zumbusch, G. R. Holtom, and X. S. Xie, Phys. Rev. Lett. **82**, 4142 (1999).
[4] M. Muller, J. Squier, C. A. de Lange, and G. J. Brakenhoff, J. Microsc. **197**, 150 (2000); M. Muller and J. M. Schins, J. Phys. Chem. B **106**, 3715 (2002).
[5] J. Cheng, A. Volkmer, L. D. Book, and X. S. Xie, J. Phys. Chem. B **105**, 1277 (2001).
[6] N. Dudovich, D. Oron, and Y. Silberberg, Nature (London) **418**, 512 (2002).
[7] J. J. Song, G. L. Eesley, and M. D. Levenson, Appl. Phys. Lett. **29**, 567 (1976).
[8] Y. Yacoby, R. Fitzgibbon, and B. Lax, J. Appl. Phys. **51**, 3072 (1980); G. Lupke, G. Marowsky, and R. Steinhoff, Appl. Phys. B **49**, 283 (1989).
[9] D. Oron, N. Dudovich, D. Yelin, and Y. Silberberg, Phys. Rev. A **65**, 043408 (2002).
[10] J. W. Goodman, *Introduction to Fourier Optics* (McGraw-Hill, New York, 1996), pp. 220–222.
[11] R. D. Schaller *et al.*, J. Phys. Chem. B **106**, 5143 (2002); T. Ishibashi and H. Onishi, Appl. Phys. Lett. **81**, 1338 (2002).
[12] D. Oron, N. Dudovich, D. Yelin, and Y. Silberberg, Phys. Rev. Lett. **88**, 063004 (2002).
[13] A. M. Weiner, Rev. Sci. Instrum. **71**, 1929 (2000).
[14] Note that this effect is not observed in the three-color experiment of Ref. [12], where it was possible to completely suppress the nonresonant background using the polarization configuration of Ref. [7].
[15] In order to match the experimental data we approximately include in these simulations off-resonant enhancement of the nonresonant process by low-lying energy levels. This is done by a slight modification of Eq. (1), where the integrand is multiplied by Ω^{-1}.